Cell Reports, Volume *40*

Supplemental information

Microglial control of neuronal development via somatic purinergic junctions

Csaba Cserép, Anett D. Schwarcz, Balázs Pósfai, Zsófia I. László, Anna Kellermayer, Zsuzsanna Környei, Máté Kisfali, Miklós Nyerges, Zsolt Lele, István Katona,Ádám Dénes

Supplemental Information

Supplemental Figures

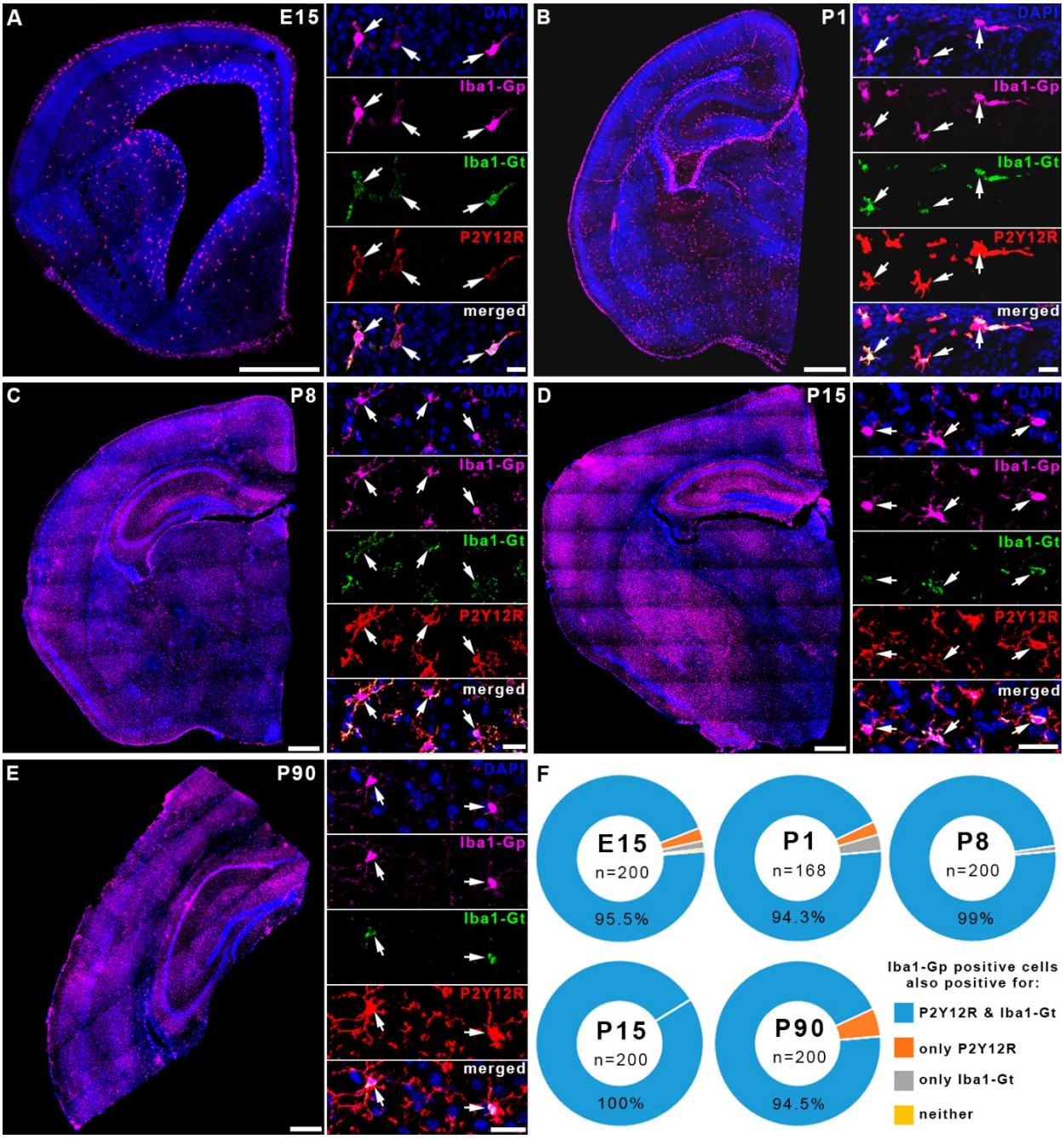

Supplemental Figure 1. Related to Figure 1. Colocalization of microglial markers during development in the mouse brain. A-E) Large montage images obtained with confocal laser scanning microscopy show the overall distribution pattern of IBA1-positive cells in mouse brains. Inserts show colocalization of markers (magenta: IBA1-guinea-pig ab., green: IBA1-goat ab., red: P2Y12R, blue: DAPI), white arrows point to microglial cell bodies. A – E15, B – P12, C – P8, D – P15, E – P90. **F)** The vast majority of IBA1-Gp positive cells were also positive for both IBA1-Gt and P2Y12R. Insert images and measurements are from the cortical plate in E15 mice, neocortex from P1-P15 mice and hippocampal dentate gyrus from P90 mice. Scale bars on large images: 500 µm, on inserts 25 µm.

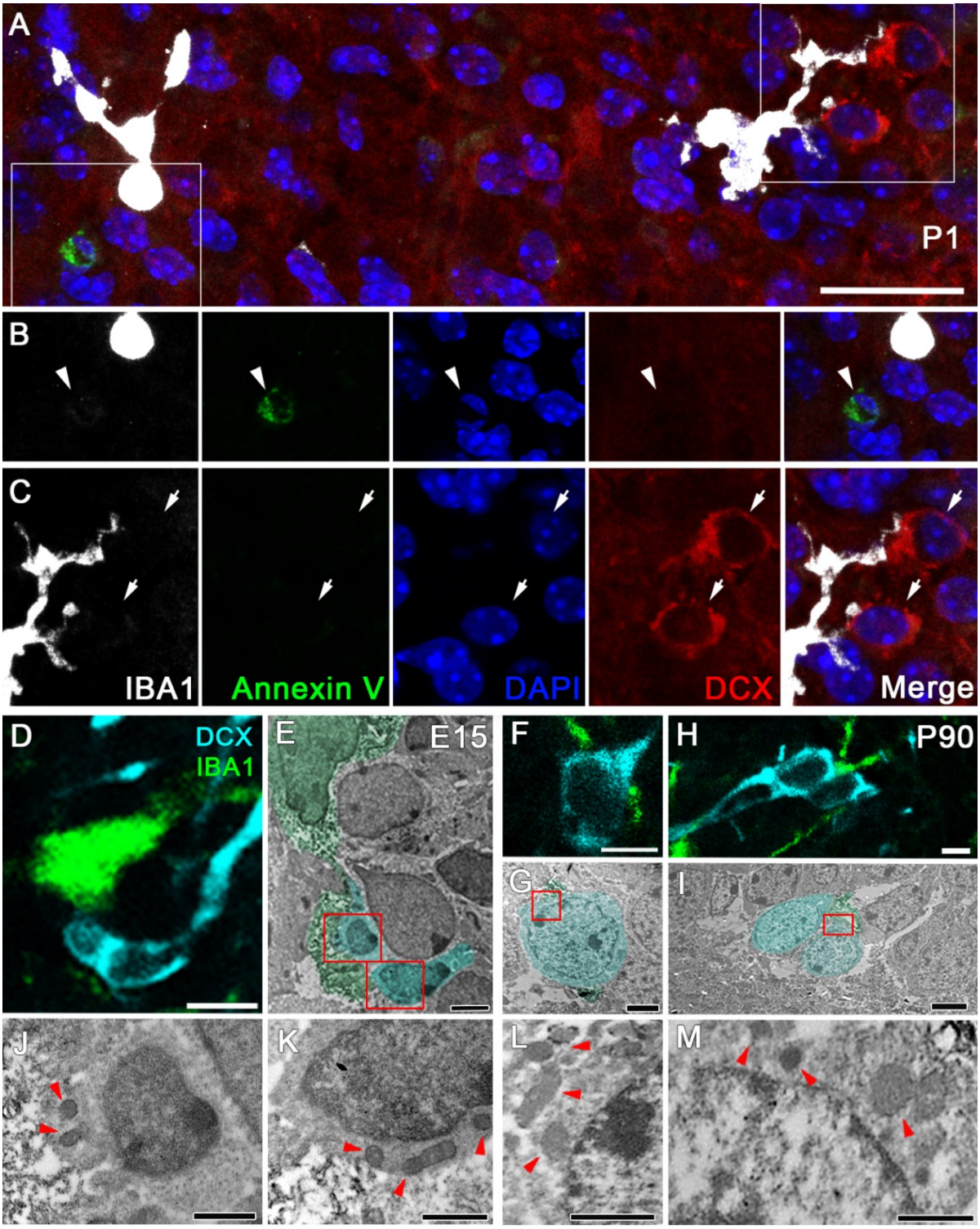

Supplemental Figure 2. Related to Figure 2. Microglial processes form direct membrane-membrane contact with cell bodies of completely healthy DCX-positive developing neurons. A) Microglia contact Annexin V-negative DCX-positive neurons (maximum intensity projection of a few image planes from a CLSM stack from a P1 mouse cortex). IBA1+ microglia are shown in white, Annexin V-positive cells are shown in green, nuclei are visualized by DAPI (blue), DCX+ neurons are shown in red. Area in the white box is shown on **B, C**. **B)** Annexin V-positive cell with partially condensed nucleus (white arrowhead). **C)** Microglia contact Annexin V-negative DCX-positive neurons, white arrow points to the nuclei of these neurons, which possess completely healthy chromatin structure. **D-M)** Maximum intensity projection of a 1.5 µm thick volume from CLSM stacks of E15 and P90 mice shows some examples of identified microglia-neuron somatic junctions. IBA1+ microglia are shown in green, DCX+ neurons are shown in cyan, contacts of CLSM-identified microglia and DCX + cells **(D, F, H)** are shown on correlated TEM images **(E, G, I)**, on which the healthy nucleus of DCX + cells is clearly visible. Somatic junction within the red box on (E, G, I), is enlarged on below **(J-M)**. Red arrowheads mark healthy neuronal mitochondria close to the junction. TEM images are pseudo-colored (microglia in green, developing neurons in cyan). Scale bar is 20 µm on **A**, 10 µm on **D**, 2 µm on **E, K, G, J,** 1 µm on **K, L, M**, 5 µm on **F, H**.

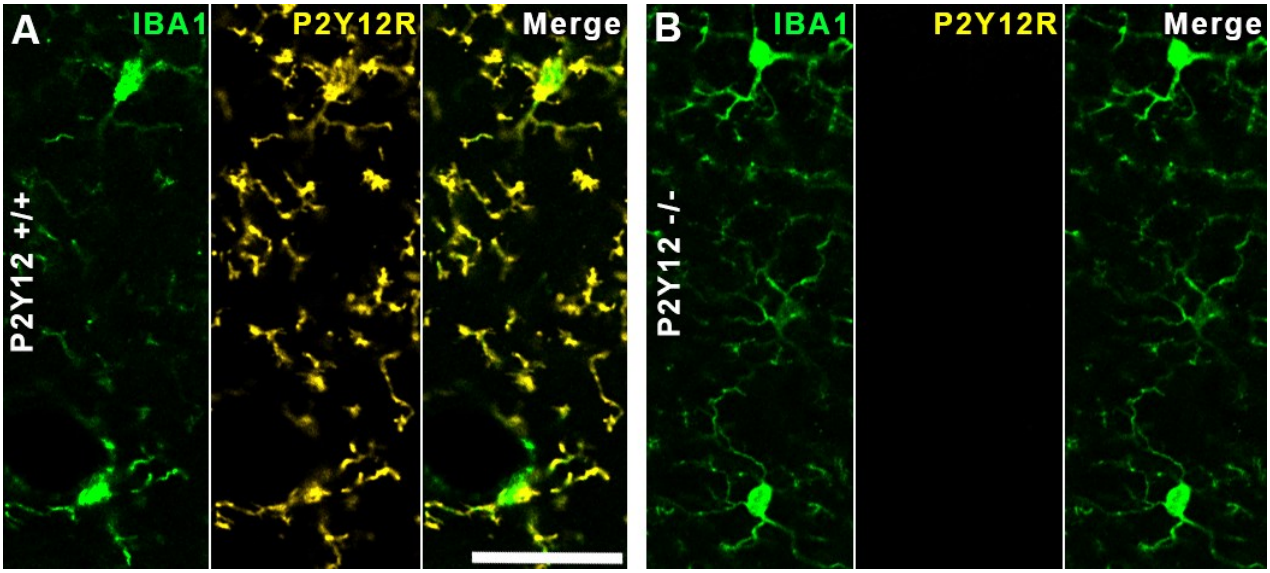

Supplemental Figure 3. Related to Figure 3. Colocalization of microglial markers IBA1 and P2Y12R in WT and P2Y12R-/- mice. A) Confocal laser scanning microscopy shows colocalization of IBA1 (green) and P2Y12R (yellow) in WT mouse brain. **B)** Same as on A, but on P2Y12R-KO mouse brain. P2Y12R-labeling is completely absent in the KO animals. Scale bar is 10 µm.

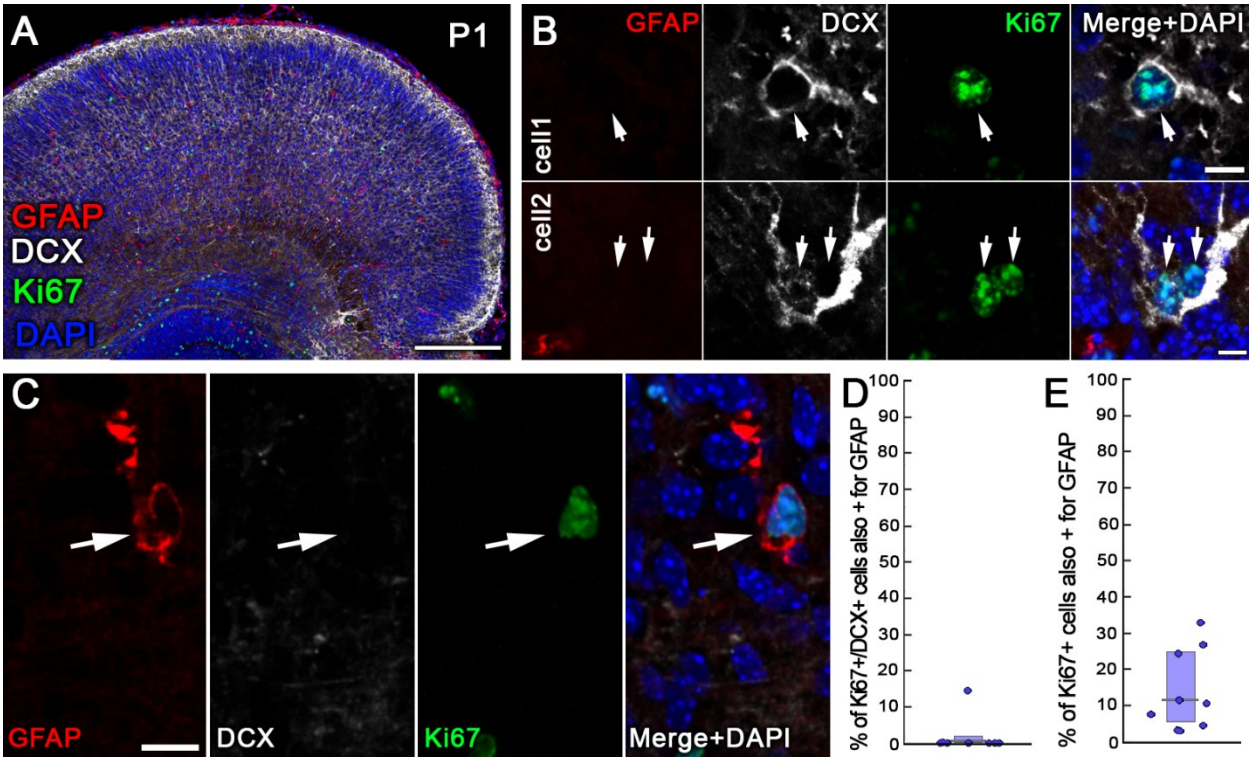

Supplemental Figure 4. Related to Figure 6. Ki67/DCX double positive cells are negative for GFAP, and only a minor fraction of Ki67+ cells express the astrocyte marker GFAP. **A)** Maximum intensity projection of a 20 µm thick volume from a confocal laser scanning microscopic stack from P1 mouse cortex. GFAP+ cells are red, DCX+ neurons are white, Ki67+ cells are green and nuclei are visualized by DAPI (blue). **B)** CLSM images show examples of Ki67/DCX double positive cells. GFAP is not expressed by these cells. **C)** CLSM images show an example of a GFAP/Ki67 double positive cell. **D)** Ki67/DCX-double positive cells are devoid of GFAP labeling (n=3 mice). **E)** Only a fraction of Ki67+ cells are also positive for GFAP as well (n=3 mice). Scale bars are 200 µm on A, 5 µm on B, and 20 µm on C.

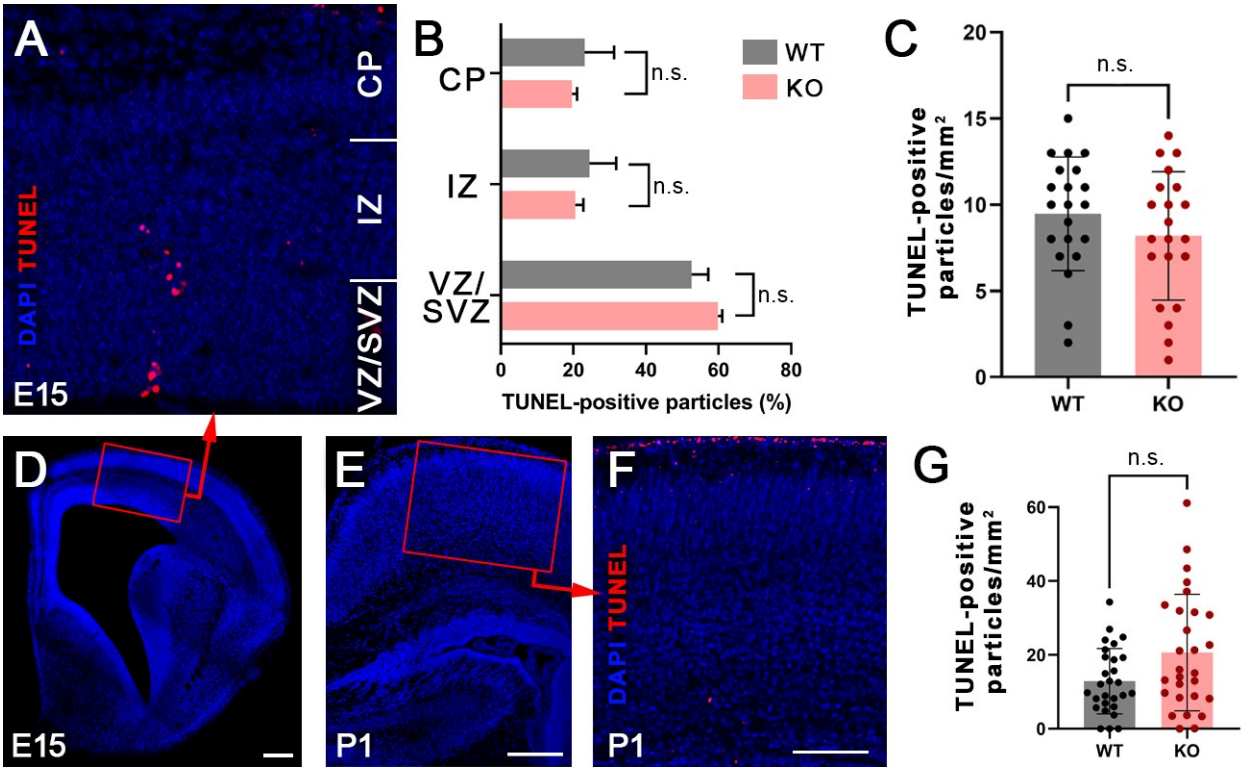

Supplemental Figure 5. Related to Figure 6. There is no detectable difference between the density of TUNEL+ cells between WT and KO (P2Y12R -/-) mouse cortex at E15 and P1. A) CLSM image shows DAPI-TUNEL double labeling on E15 mouse cortex. **B)** Percentage of TUNEL-positive particles throughout cortical layers in WT and KO mice at E15 (n=3-3 mice). **C)** Density of TUNEL-positive particles does not differ in WT and KO mice (3-3 mice). Unpaired t-test; n.s. no significant difference. **D)** CLSM image shows DAPI-labeled E15 mouse brain hemisphere, red box marks area of measurement. **E)** CLSM image shows DAPI-labeled P1 mouse brain cortical region, red box marks area of measurement. **F)** CLSM image shows DAPI-TUNEL double labeling on P1 mouse cortex. G) Density of TUNEL-positive particles does not differ in WT and KO mouse cortex at P1 (3-3 mice). Unpaired t-test; n.s. no significant difference. Scale bars are 200 µm on D, E, 100 µm on F (also for A).

Supplemental Tables

Supplemental Table 1. Microglial contact prevalence on DCX+ cells. Related to Figure 1. I-P.

Microglial contact prevalence on DCX+ cells					
	∑ contact	**soma**	**prox.tuft**	**both**	**n (cells)**
E15	35.20%	27.50%	5.60%	2.10%	142
P1	36.40%	25.80%	6.10%	4.50%	132
P8	61.90%	44.70%	9.50%	7.70%	168
P15	97.20%	62.30%	6.60%	28.30%	106
P90	92.50%	35.80%	14.20%	42.50%	106

Supplemental Table 2. Mitochondrial enrichment at contact sites. Related to Figure 2. O-S.

TOM20 fluorescent intensity comparison					
	non-contact (median, interquartile)	**contact (median, interquartile)**	**difference**	**p value**	**n (contacts)**
E15	**0.32**, 0.22-0.42	**0.13**, 0.09-0.15	146.00%	p<0.001	30
P1	**0.3**, 0.23-0.43	**0.09**, 0.05-0.13	233.00%	p<0.001	30
P8	**0.3**, 0.19-0.42	**0.09**, 0.06-0.13	233.00%	p<0.001	33
P15	**0.3**, 0.21-0.36	**0.08**, 0.05-0.12	275.00%	p<0.001	30
P90	**0.22**, 0.15-0.31	**0.1**, 0.06-0.15	120.00%	p<0.001	41

Supplemental Table 3. P2Y12R enrichment at contact sites. Related to Figure 3. G.

Percentage of P2Y12R labeling				
Age	quarter	median	1st quartile	3rd quartile
E15	1st	53%	39%	81%
	2nd	29%	8%	44%
	3rd	15%	3%	22%
	4th	0%	0%	6%
P1	1st	44%	34%	50%
	2nd	24%	14%	39%
	3rd	9%	4%	21%
	4th	8%	0%	22%
P8	1st	38%	36%	100%
	2nd	26%	0%	42%
	3rd	16%	0%	19%
	4th	0%	0%	2%
P15	1st	53%	47%	72%
	2nd	30%	27%	36%
	3rd	8%	0%	21%
	4th	0%	0%	2%
P90	1st	46%	37%	51%
	2nd	32%	28%	38%
	3rd	18%	10%	27%
	4th	1%	0%	10%